Title: Cornea Confocal Microscopy: utilities and perspectives.

Author: Eduardo Rojas Alvarez, PhD.

Institution: University of Cuenca, Ecuador. Ophthalmological Center Exilaser. Ecuador.

drerojasalvarez@gmail.com

Abstract

The cornea is the ocular refractive medium with the greatest refractive power of the eye. The study of it is of vital importance for the diagnosis and follow-up of ophthalmological diseases with the aim of achieving high standards of visual acuity in our patients. Confocal microscopy of the cornea allows in-depth study of it, quickly, safely, painlessly, obtaining high-resolution images of the corneal sublayers. This chapter summarizes the procedure for performing corneal confocal microscopy, the normal characteristics of the tissue with real images of our patients, as well as a brief explanation of the main applications of this technology in the study of corneal dystrophies (keratoconus), in refractive surgery, corneal transplantation, infectious keratitis, glaucoma filtration bulla, among other topics.

Key words: microscopía confocal, cornea, epitelio, estroma, endotelio.

1. Introduction

The sense of vision is one of the most precious, the study of the visual phenomenon has always been in the sights of researchers at all times, with the common goal of finding the necessary tools to diagnose and treat ophthalmological disorders in a timely manner and therefore, achieve better results of visual acuity in patients.

Within the eyeball, one of the most important anatomical elements in terms of visual contribution is the cornea. This tissue is part of the outermost layer of the eyeball, it is made up of 5 layers, has a thickness in the central part of 0.5 mm and is thicker in the peripheral part. It is avascular and confers most of the ocular diopter power.In ophthalmology consultations, corneal diseases are a frequent reason for consultation, since they are the cause of decreased visual acuity. There are different diagnostic methods used by the ophthalmologist to study the cornea, such as: anterior biomicroscope, corneal topography, fluorescein staining, endothelial microscopy, keratometry, among others.

The advent of confocal microscopy has made it possible to study the corneal sublayers in greater depth, in vivo, without discomfort and with rapid obtaining of high resolution images. The principle of confocality has been very useful for the study of corneal dystrophies, patients with corneal refractive surgery, corneal infections, contact lens users, corneal transplantation, among other applications. All these results have positioned confocal microscopy as a method of great diagnostic importance in the study of the human cornea, aspects that we will summarize in the current chapter.

2: DEVELOPMENT

2.1 General principles of cornea confocal microscopy.

Until recently, the diagnosis of diseases of the cornea and the ocular surface has been based on the traditional anterior biomicroscopy. The exponential evolution of technology that has occurred in the last two decades has been led by the introduction of new instruments such as corneal topography, ultrasonic biomicroscopy and optical coherence tomography, among others, for the analysis of the ocular anterior segment. [1-3]

These techniques offer details of the corneal curvature or macroscopic sections for the examination of structures. On the other hand, the microscopic morphology of the ocular surface was only performed by ex vivo histology, which presents limitations such as tissue degeneration, the presence of artifacts and the impossibility of evaluating the processes of disease.

Confocal microscopy is a non-invasive method for the study of microscopic images in living tissues, which has been used for the investigation of corneal microstructure since the beginning of the 1990s.[4-6] The study of images has evolved from experimental levels in laboratory research, to applications in healthy and sick patients. [7,8]

The confocal microscope for the study of cells of the nervous system in vivo, original from 1955, it was developed by Minsky in 1988. This allowed optical theory to be more formally developed and extended in the years of that decade (Wilson and Sheppard, 1984) and in the following decade (Hill; Masters and Thaer, 1994).[9,10] The basic principle of confocal microscopy is that an isolated point of

tissue can be illuminated by a beam of light and simultaneously captured by a camera in the same plane. This produces a high resolution image. [7, 10-13]

Currently, there are several types of confocal microscopes, for example: the Confoscan P4 (Tomey, United States), the Confoscan 4 (Nidek, Japan) and the confocal corneal laser microscope (Heidelberg Retina Tomograph II Rostock Corneal Module: HRTII) (Heidelberg, Germany), among others.[3, 14,15]

All confocal microscopes have the same basic principles of operation.8, 10 Light passes through an aperture and is focused on an objective lens in a small area. Light is reflected from this area and passes through a second objective lens. This light is focused on a second aperture, the out-of-focus light is eliminated. Illumination and detection are in the same focal plane, therefore the term confocal is used.[10,16-19]

The system has the ability to discriminate high-resolution lateral and axial images of light that is not in the focal plane, compared to light microscopes. Clearly as a system it is limited by a small field view. Image quality generally depends on two factors: contrast and resolution. It also depends on the numerical aperture of the objective lens, illumination levels, and the reflectivity of the studied structures and the wavelength of the illumination source.[8, 14] (Figure 1,2)

2.2. - The normal cornea by confocal microscopy.

The superficial epithelium of the cornea is observed as hexagonal cells with bright edges with a defined nucleus and homogeneous cytoplasm.[20-22] The cells have a characteristic polygonal shape, almost hexagonal, which are characterized by a highly reflective cytoplasm since they are in a high continuous flaking process, with a shiny core and space perinuclear dark clearly visible. The superficial epithelium is five microns thick. [11, 22-26] (Figure 3)

Intermediate stratum cells are characterized by bright edges and dark cytoplasm. The nucleus can be distinguished with great difficulty.[27-29] The average density is approximately 5000 cells / mm² in the central cornea and 5,500 cells / mm² in the periphery. The cells of the middle stratum have the lowest reflectivity in the entire corneal epithelium.[12, 22, 30, 31]

The basal cells are located immediately above Bowman's membrane. They present bright cell borders in which the nucleus is not visible.[7, 12, 23, 32-34] Comparison between cells reveals inhomogeneous reflectivity of the cytoplasm. Like the cells of the intermediate stratum, basal cells show only minimal variation in their shape and size. In terms of cell density in normal subjects, the ratio of surface, intermediate, and basal cells is 1: 5: 10. Basal cells have 10-15µm in diameter and form a regular mosaic with dark cell bodies and brightness at the cell edges. [14, 35] (Figure 4)

Langerhans cells appear as bright corpuscular particles with dendritic cell morphology and a diameter of 15 mm. Their distribution is in the form of a gradient from low numbers in the center to high cell densities in the periphery of the cornea.[30, 36, 37]

The subbasal nerves are located between Bowman's membrane and the basal epithelium.38-40 They appear as linear structures with homogeneous reflectivity, a dichotomous Y-shaped appearance, and fine H-shaped interconnecting fibers.[7,40,41] The membrane of Bowman is not visible by microscopy confocal. The subepithelial plexus is located between Bowman's membrane and the anterior stroma. This

plexus has a diffuse, patchy distribution, apparently limited to the midperipheral cornea and probably absent in the central cornea. [40, 42-47] (Figure 5)

The stroma is seen with images of keratocyte nuclei. The cell body, keratocyte processes, and stromal collagen are not usually visible on the normal cornea. Keratocytes in the anterior stroma are well-defined images with brightness, oval, objects with varied orientation that contrast with a dark background.[46, 48-51] In the middle stroma, keratocytes have a more regular oval shape. Keratocytes in the posterior stroma appear more elongated than those in the anterior layers. [22, 45, 51,52] (Figure 6,7)

Stromal nerves are located in the anterior and middle stroma, but they cannot be visualized in the posterior stroma: they appear as linear, thin, reflective structures, in various orientations, with a dichotomous pattern; internal details of the nerves are not observed.[53- 58]

Descemet's membrane is not visible. Endothelial cells appear as a regular hexagonal cell line exhibiting bright cell bodies with darker edges. [8,37,52,59-62] (Figure 8)

Taking as a reference the characteristics of the normal cornea, some variables have been described after corneal refractive surgery, through confocal microscopy, such as: the thickness of the epithelium[27] and the corneal flap[16], the keratocyte cell density in different strata[50], the characteristics of corneal nerves[41], endothelial cell density, pleomorphism, polymegatism[60], corneal haze thickness[29], among other variables. (Figure 9,10)

2.3- Applications of confocal microscopy of the cornea

Evaluation of cross linking treatment

Confocal microscopy is a diagnostic means that allows the monitoring of histological modifications that occur due to the effect of corneal crosslinking. It allows to show the recovery of the tissue in the follow-up period of the treated cases.

Among the findings, a rarefaction of keratocytes accompanied by stromal edema in the first month can be observed in the anterior-middle stroma; This can take the appearance of a trabecular network, where small elongated keratocyte nuclei can be detected corresponding to masked necrotic keratocytes and apoptotic bodies, respectively. Initial restocking generally occurs within 3 months at this depth and they regenerate almost completely within 6 months.[63]

Corneal transplant

In confocal microscopy, we observed, in most transplanted corneas, loss of continuity of corneal nerves, absence of nerve fibers, and reduction and activation of keratocytes. When confocal microscopy findings were related to the transparency status of the graft, the absence of nerve fibers was observed in all cases of non-transparent cornea and in the vast majority of transparent corneas.[64]

Corneal dystrophies

Sometimes it is difficult to make the differential diagnosis between different types of corneal dystrophies using only slit lamp biomicroscopy, hence the importance of confocal microscopy in the study of dystrophies.

For example, in a patient with a diagnosis of basement membrane dystrophy, reduplication of the basement membrane is observed, in Meesmann's dystrophies hyporeflectic areas in the basal layer of the epithelium, mostly circular, oval or drop-shaped, with a range of 48 and 145 µm in diameter. [65]

In Thiel-Behnke dystrophy, deposits are observed in the basal layer of the corneal epithelium of homogeneous reflectivity with curved filaments accompanied by dark shadows. Meanwhile, in corneas with Reis-Bücklers dystrophy, in the same layer, deposits with extremely high reflectivity are observed from small granular materials.[65]

In granular dystrophy by confocal microscopy, the superficial epithelium is normal in appearance, while in the basal epithelium, highly reflective deposits are observed without defined borders. High reflectivity deposits are also observed in the superficial stroma. At Bowman's membrane level, sub-basal nerves with a raised fundus can be seen.[65]

In keratoconus, the epithelium shows the following characteristics: elongated, spindle-shaped surface cells, larger and irregularly spaced nuclei of wing cells, and flattened basal cells. Images obtained using confocal microscopy reveal the disruption of Bowman's layer and the occasional presence of epithelial cells and stromal keratocytes. [65]

Corneal refractive surgery

The confocal microscope has been widely used in the study of patients after refractive procedures. Modifications have been described at the level of different sublayers of the cornea, showing high reliability and reproducibility for these purposes. [66-69]

Confocal microscopy allows the visualization of the stromal flap in LASIK, the analysis of its thickness and regularity, the density of corneal cells by stromal sublayers, the exact obtaining of the residual corneal bed, the study of the modifications of the subbasal nervous plexus and the nerves, stromal cells, as well as their recovery after this surgery. It allows the study of corneal haze in PRK, its evolution and response to treatment.[66-69] (Figure 11-19)

Infectious keratitis

Confocal microscopy is emerging as an important technique in the early diagnosis of various corneal entities. It is capable of providing magnifications close to 200x-500x, providing images with high detail and contrast levels, even in opacified corneas. Its non-invasive nature makes it an especially useful technique in the diagnosis of infectious keratitis caused by Acanthamoeba. In addition, it allows

repeated examinations, which helps the diagnosis, monitoring and taking therapeutic attitudes. Typical lesions correspond to amoebic cyst or trophozoite (hyperreflective lesions surrounded by a double wall and a peripheral halo), and radial keratoneuritis (linear hyperreflective thickening). Therefore, when faced with a patient who develops nonspecific manifestations of infectious keratitis, the possibility of performing this test should not be forgotten, in conjunction with histological studies, since it gives us the possibility of an early diagnosis and a better prognosis.[70]

Patients with retinal surgeries

We can inspect corneal morphology at the cellular level in patients with emulsified silicone oil in the anterior chamber, which contributes to detecting early histological changes, both morphological and morphometric that guide us towards a behavior to avoid subsequent tissue damage.

Images obtained through confocal microscopy show different degrees of polymegatism and pleomorphism, hyperreflectivity determined by deposits of emulsified silicone oil on the corneal endothelium that are seen as bright or elongated stippling, activation of keratocytes in the stroma with loss of the matrix extracellular by contact with oil, multidots lesions and in some cases folds of the descemet.[71]

Diabetic patients

Diabetes mellitus is the most common endocrine disorder in ophthalmic practice, and disorders of the anterior segment are less frequently described than those of the retina, although they are present in many patients. This disease affects the biomechanics of the corneal epithelium and endothelium, causes a significant effect on the morphology, metabolism and clinical and physiological aspects of the cornea. The metabolic disorders typical of diabetics constitute an important factor in the appearance of diabetic neuropathy and other subsequent pathologies.

In confocal microscopy, a decrease in the density of the sub-basal nerve plexus can be observed with an increase in its thickness and tortuosity, a decrease in the density of the nerve fibers of the sub-basal nerve plexus, as well as the association of certain changes morphological of these as: fewer branches, shorter lengths, as well as increased tortuosity and presence of edema.

Greater total corneal thickness and layers are observed, the basement membrane is visible in diabetic patients. There is a decrease in the sub-basal nervous plexus with vertical disposition and an increase in the tortuosity of the nerve fibers.[72]

Filtering bull in glaucoma.

The confocal scanning laser microscope with the Rostock corneal module is a revolutionary element in the monitoring of glaucoma operated patients. The presence of encapsulated stromal cysts surrounded by a hyperreflective line that defines them and separates them from the rest of the structures (capsule) can be evaluated. Besides the visualization of thick conjunctival vessels that describe curves in their course (tortuous); On the other hand, the size of the filtering bullet

is evaluable, through the measurement of the dimensions of the bullet in its largest diameter. [73]

2.4- Method of use of the corneal confocal microscope. Calculations and images obtained.

The NIDEK ConfoScan four confocal microscope is shown for obtaining and studying in vivo images of corneal tissue. The Z ring must be attached for fixation of the eyeball with the 40x lens. It is programmed in automatic scanning mode, with central fixation, image acquisition speed of 25 images per second, 500x magnification, 0.6 µm / pixel lateral resolution, with 350 images per scan, 1.98 mm working distance.

Anesthetic eye drops and subsequently Viscotears (gel) are instilled as a coupling medium between the cornea and the Z ring. The lens is advanced until the ring is contacted with the coupling substance. The objective lens is aligned with the center of the cornea until the first images of corneal epithelium are observed. The digital images obtained are captured automatically and recorded on a computer for later analysis. Before and after each examination, the objective lens is cleaned with isopropyl alcohol.

Each image obtained is separated from the adjacent image by four microns, 25 µm depth of field, intensity level 0 to 255, Z-ring pressure 20%. All shots belong to the central four mm of the cornea.

The necessary examinations are performed in each patient until obtaining, by full-focus quantitative confocal microscopy (CMTF curve), scans and images of maximum stability in terms of pressure applied by the Z ring with variations of less than 10%, represented by the yellow curve. The selected images should not be modified in brightness and contrast, the analysis is carried out with the NAVIS software.

Figure 1: NIDEK ConfoScan 4 confocal microscope.

Steps to follow in microscopy. A: Z ring for fixation of the eyeball. B: 40X lens. C: Coupling of A and B. D: The lens was advanced until contacting the ring with the coupling substance for examination.

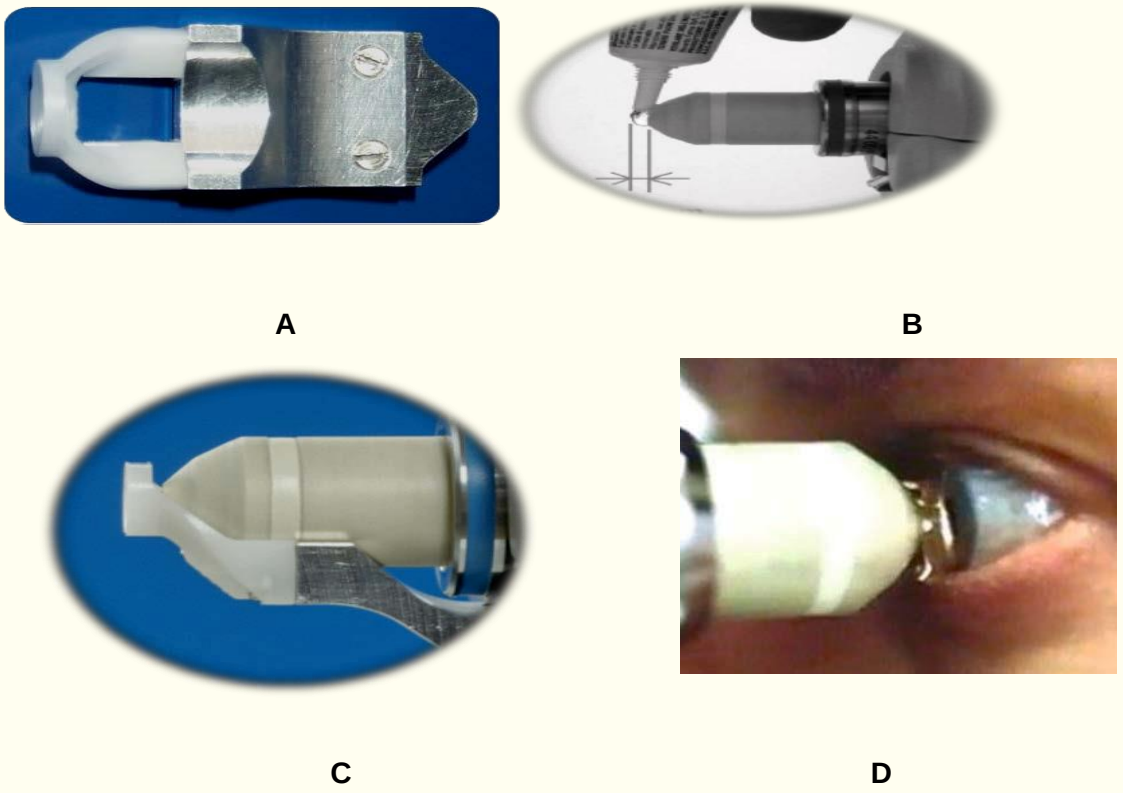

Figure 2: Full focus quantitative confocal microscopy (CMTF), where the selected image is seen in the upper right: Apical epithelium one year after LASIK. The top left shows the parameters of depth, distance, intensity level, pressure of the Z ring, among others.

The lower right part shows the quality of the shot given by the constancy of the yellow line and the uniformity of the white line. The green line corresponds to the reflectivity in the form of peaks. An image of corneal epithelium belonging to the first image of the 4 existing ones is shown.

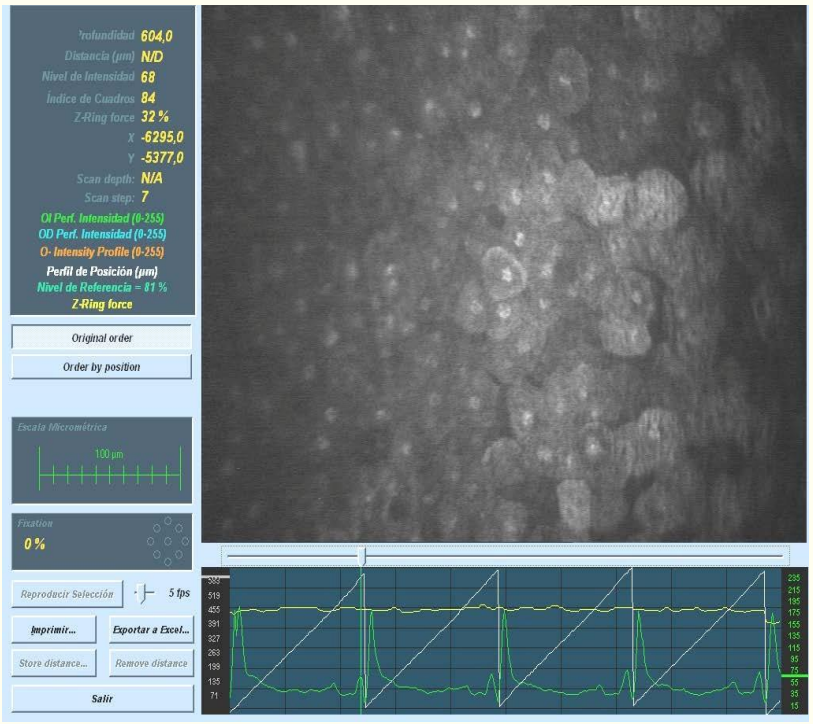

Figure 3: Apical corneal epithelium: Layer of polygonal cells with defined edges, with a bright nucleus that stands out from the homogeneous cytoplasm. Corresponds to patient 6 months after PRK.

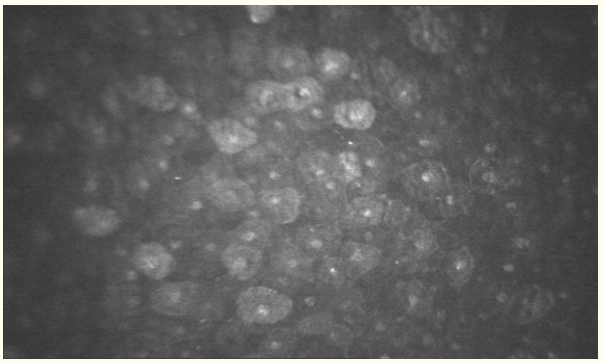

Figure 4: Basal corneal epithelium: layer of cells with darker homogeneous cytoplasm lacking a nucleus and defined borders. Corresponds to patient per year of PRK.

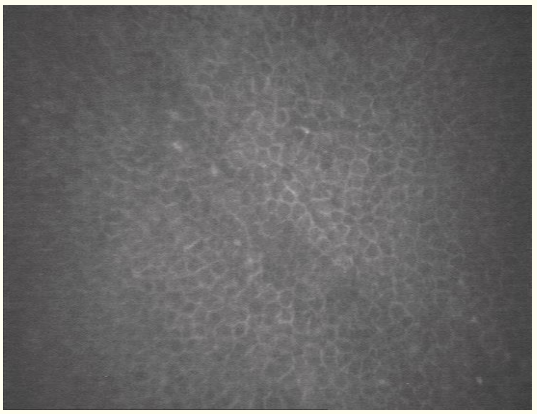

Figure 5: Subbasal nerve plexus: Nerve fibers contrasting against the dark background, thin, bright, distributed in a parallel or oblique fashion with various interconnecting bifurcations. Corresponds to patient at LASIK year.

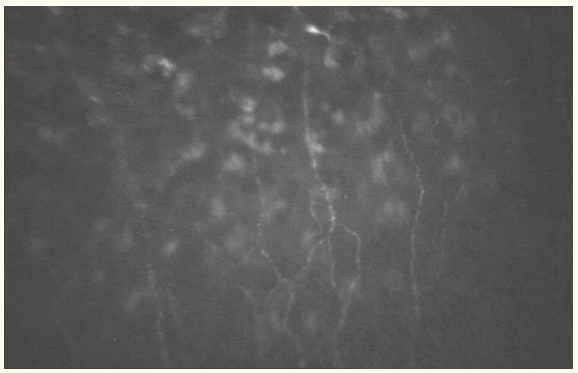

Figure 6: Corneal stroma: Defined by the presence of bright oval bodies (keratocytes) that contrast against the dark background. Corresponds to patient 3 months after LASIK.

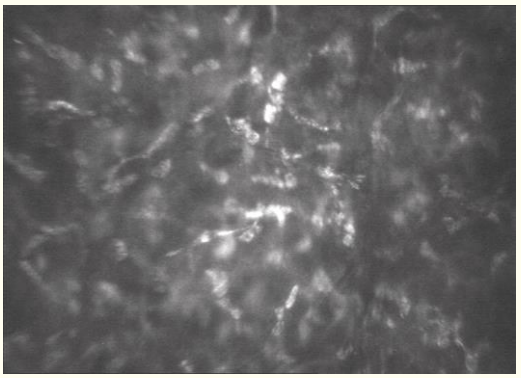

Figure 7: Surgical interface: Presence of bright pinpoint bodies that stand out against the dark background. Corresponds to patient 1 month after LASIK.

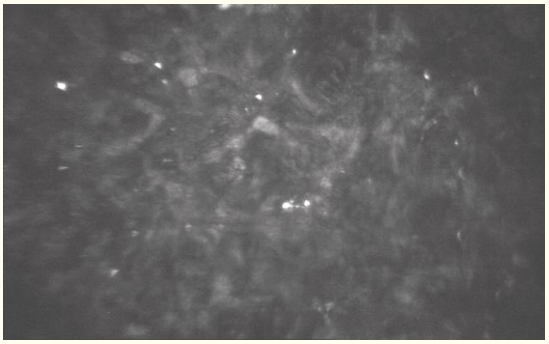

Figure 8: Corneal endothelium: Hexagonal cells with defined edges, anucleated, with homogeneous cytoplasm. Corresponds to patient per year of PRK.

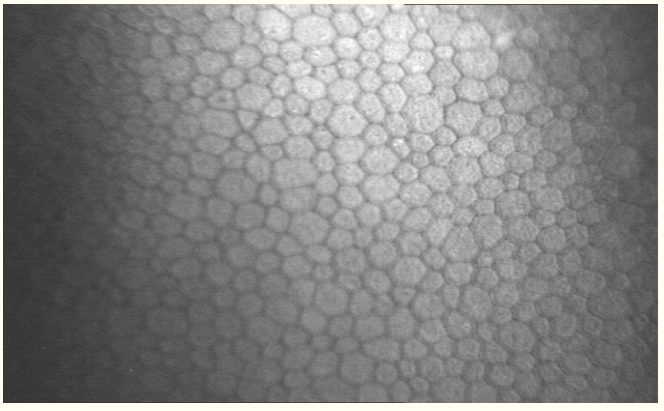

Figure 9: Corneal haze, the keratocyte limits cannot be defined, with greater brightness than the rest of the stromal images. Corresponds to patient 3 months after PRK.

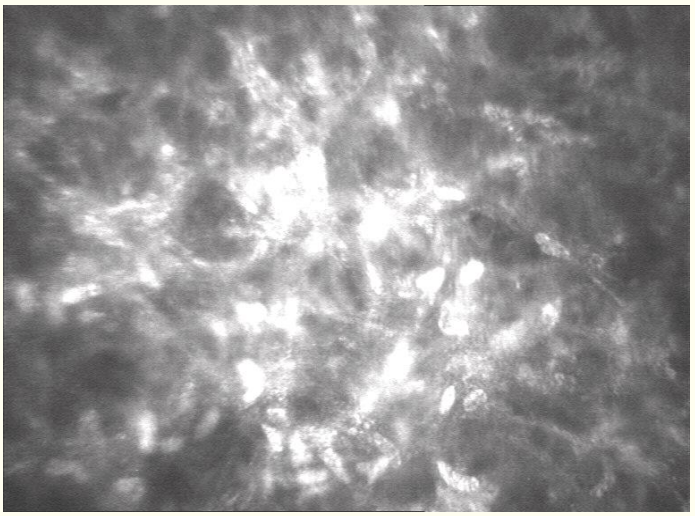

Figure 10: Pachymetry measurement. Pachymetry is the value illustrated as depth in the upper left of the CMTF curve image. The example is 6 months after LASIK.

Full focus quantitative confocal microscopy (CMTF), where the selected image is seen in the upper right: Apical epithelium one year after LASIK.
The top left shows the parameters of depth, distance, intensity level, pressure of the Z ring, among others. The lower right part shows the quality of the shot given by the constancy of the yellow line and the uniformity of the white line. The green line corresponds to the reflectivity in the form of peaks. An image of corneal epithelium belonging to the first image of the 4 existing ones is shown.

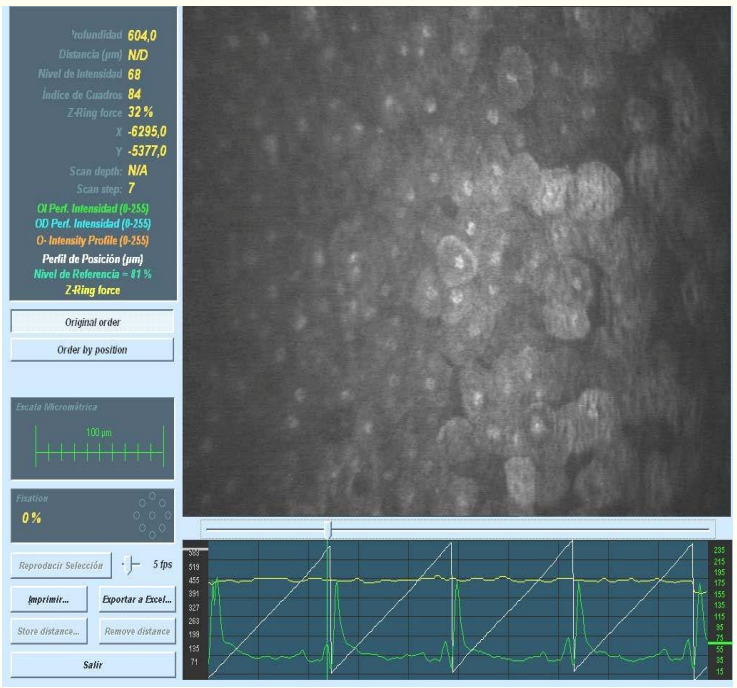

Figure 11: Measurement of epithelial thickness. The most anterior apical corneal epithelium image is selected by CMTF curve (upper image) and the cursor is moved to the last basal corneal epithelium image. (lower image) Epithelial thickness is the value illustrated as Distance (µm) = 41 in the upper left of the lower image. The example is 6 months after LASIK.

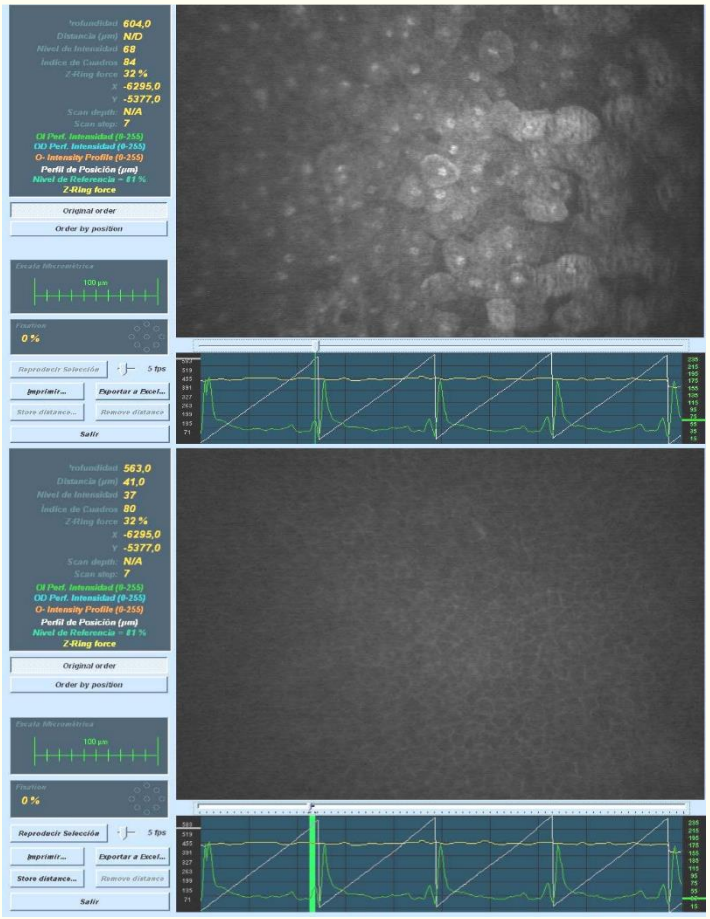

Figure 12: Flap thickness measurement. The first apical corneal epithelium image (upper image) is selected on the CMTF curve and the cursor is moved to the first surgical interface image (lower image). The thickness of the flap is the value illustrated as Distance (µm) = 147 in the upper left of the lower image. The example is 6 months after LASIK.

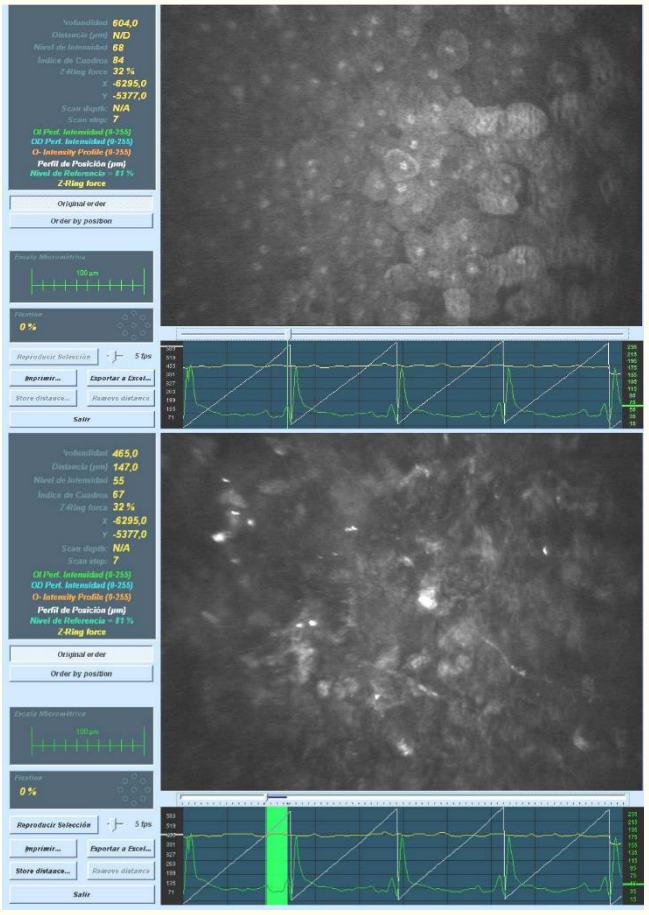

Figure 13: Measurement of residual stromal bed (3 months after LASIK). Using the CMTF curve, the last surgical interface image (upper image) is selected and the cursor is moved to the last image of corneal endothelium (lower image). The residual stromal bed thickness is the value illustrated as Distance (µm) = 439.0 in the upper left of the lower image. The example is 3 months after LASIK.

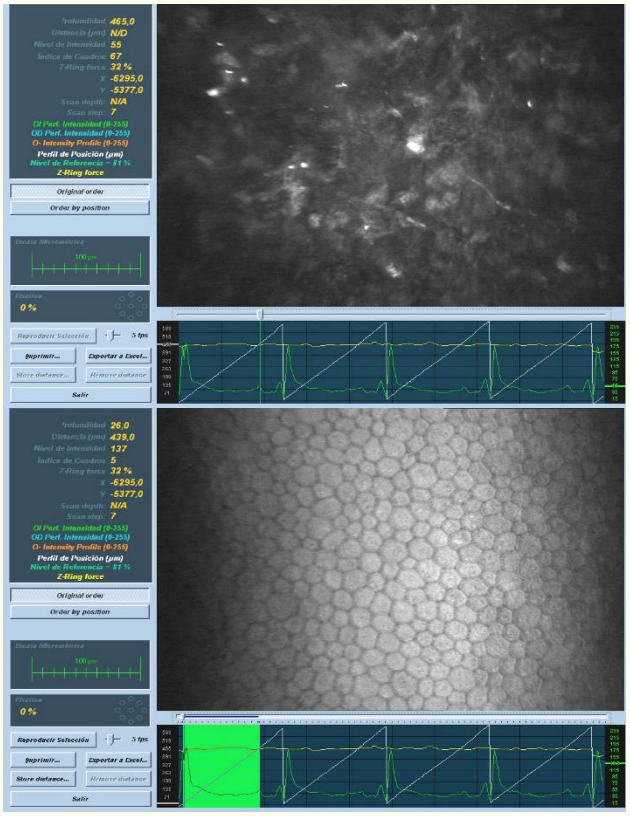

Figure 14: Calculation of the cell density of the apical epithelium. After selecting the image and the ROI area (0.0500 mm²), the cells are marked in the upper left image and the density value is obtained through the software, in this case 937.6 cells / mm². The example corresponds to 6 months after PRK)

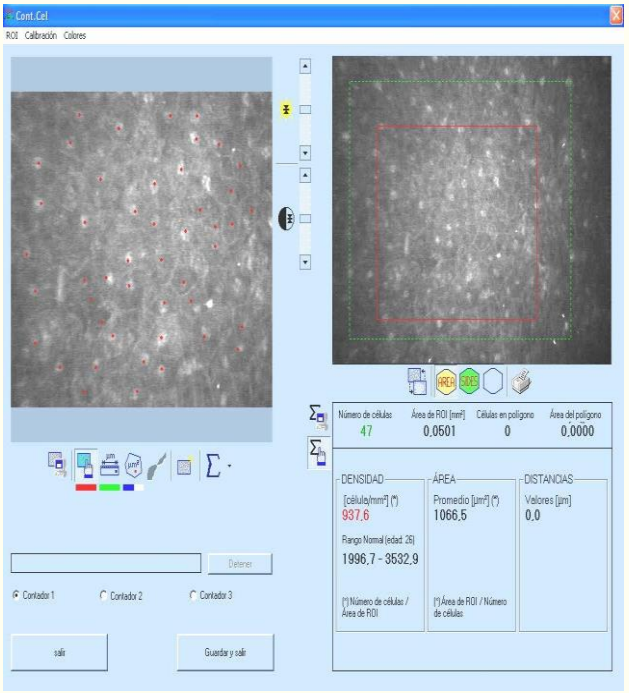

Figure 15: Calculation of basal epithelium cell density. After selecting the image and the ROI area (0.0500 mm²), the cells are marked in the upper left image and the density value is obtained through the software, in this case 4642 cells / mm². Example corresponds to 1 year after PRK)

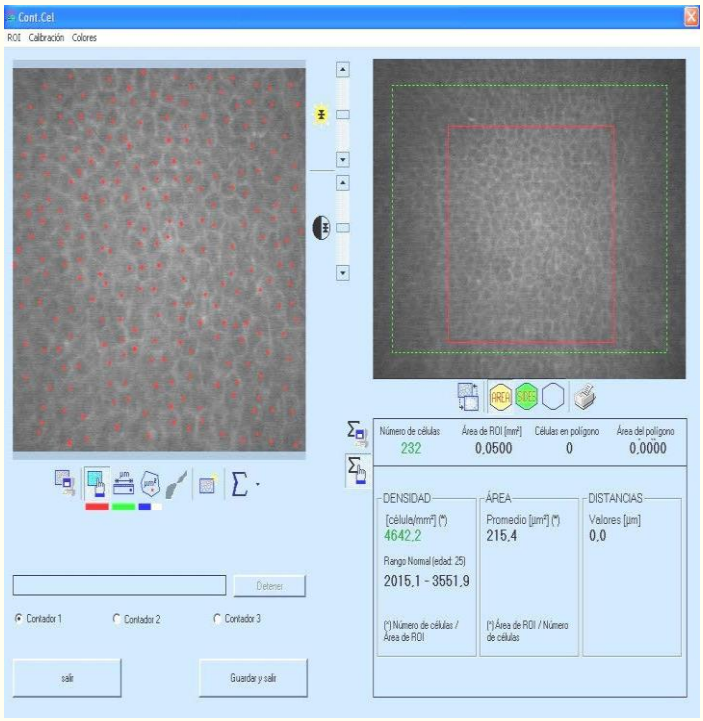

Figure 16: Calculation of keratocyte density. In the upper right portion the selection of the area is observed, in the upper left portion the marking of each keratocyte.

The first density quotient obtained is the one with red letters. This value is divided by the effective depth of field of the equipment: 25 to obtain the density in cells / mm^3

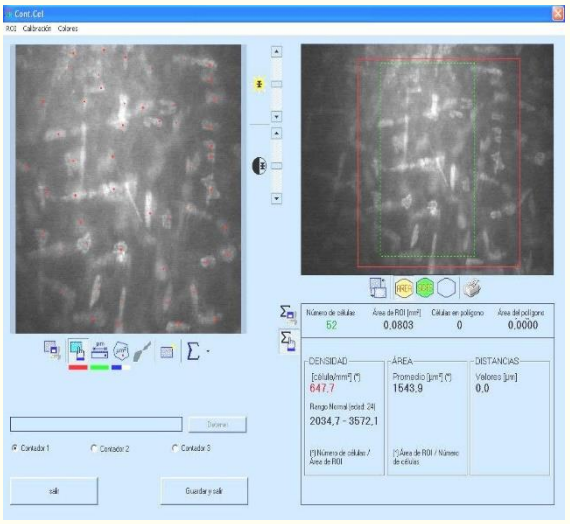

Figure 17: Calculation of endothelial variables. In the upper right portion the selection of the area is observed, in the upper left portion the automatic marking of the cells. In the lower portion, the values obtained for endothelial cell density, pleomorphism and polymegatism are observed.

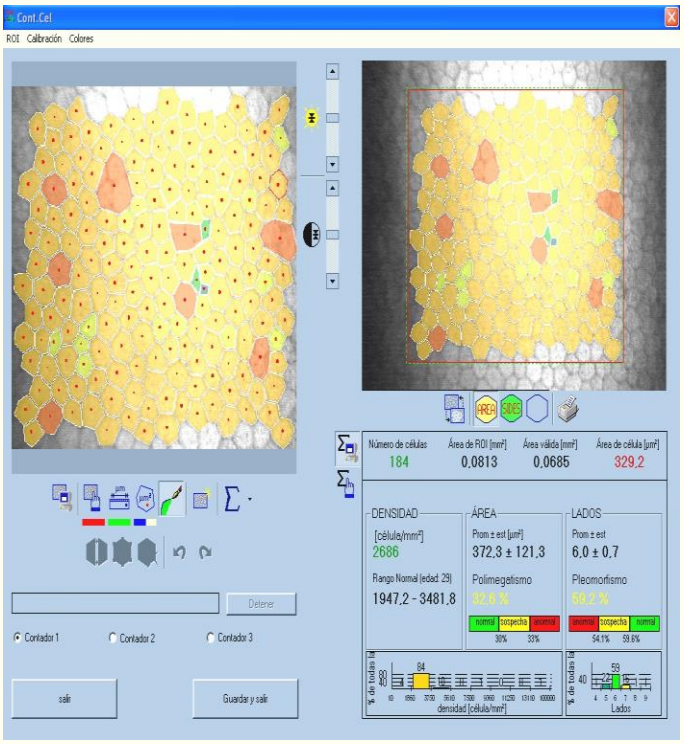

Figure 18: Measurement of corneal haze, after PRK. In this case, 3 months after PRK, the upper image shows a CMTF curve, taking the first image of corneal haze, then the cursor is moved to the last image of corneal haze shown in the lower figure, where the parameter called distance = 61 µm.

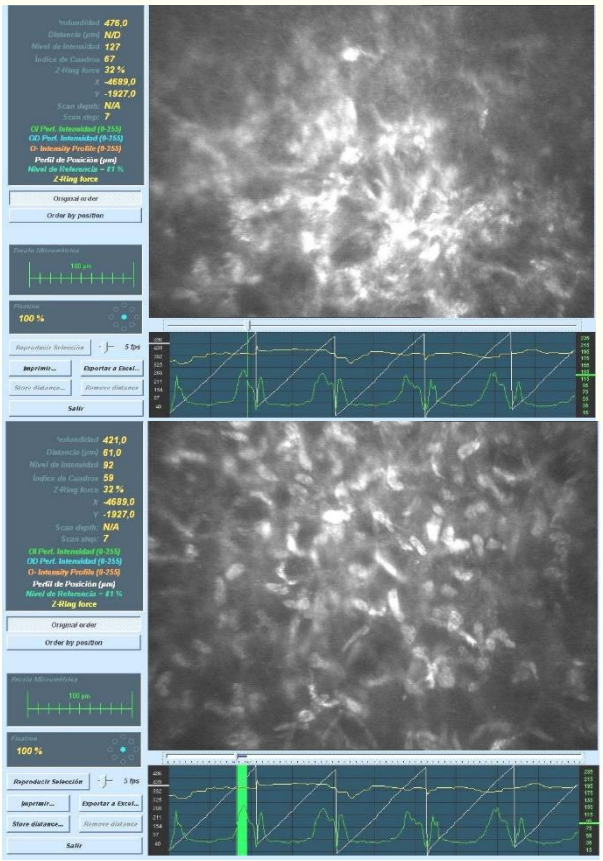

Figure 19: Subbasal nerve plexus. A: Short nerve, less than 200 µm in length. B: Long nerve (greater than 200 µm without interconnections). C: Nerves long with interconnections. D: Measurement of the nerve.

A

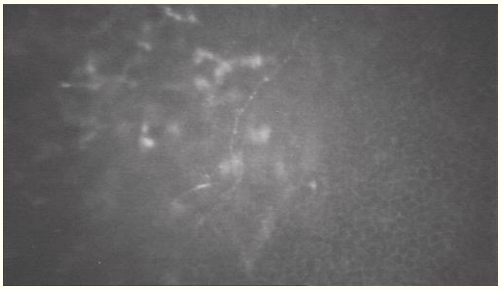

B

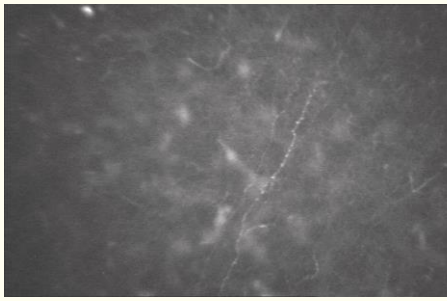

C

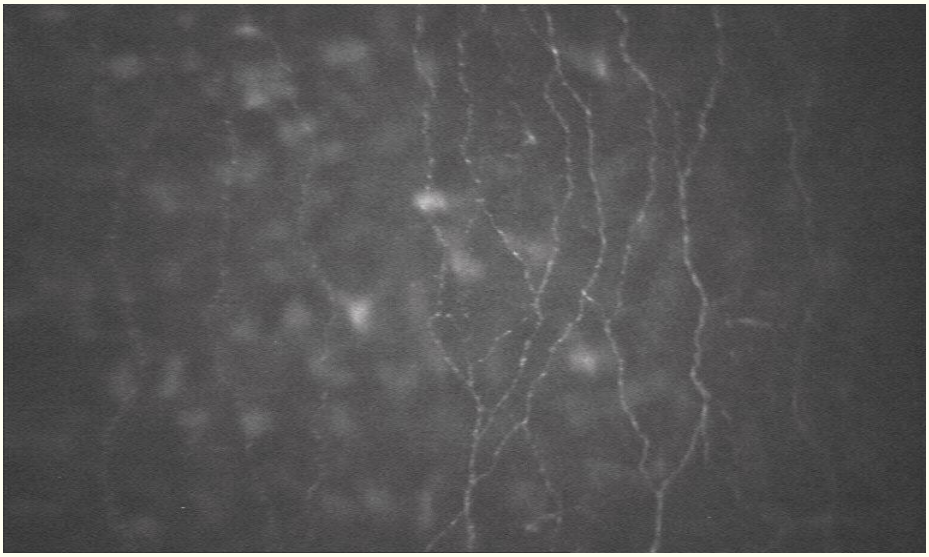

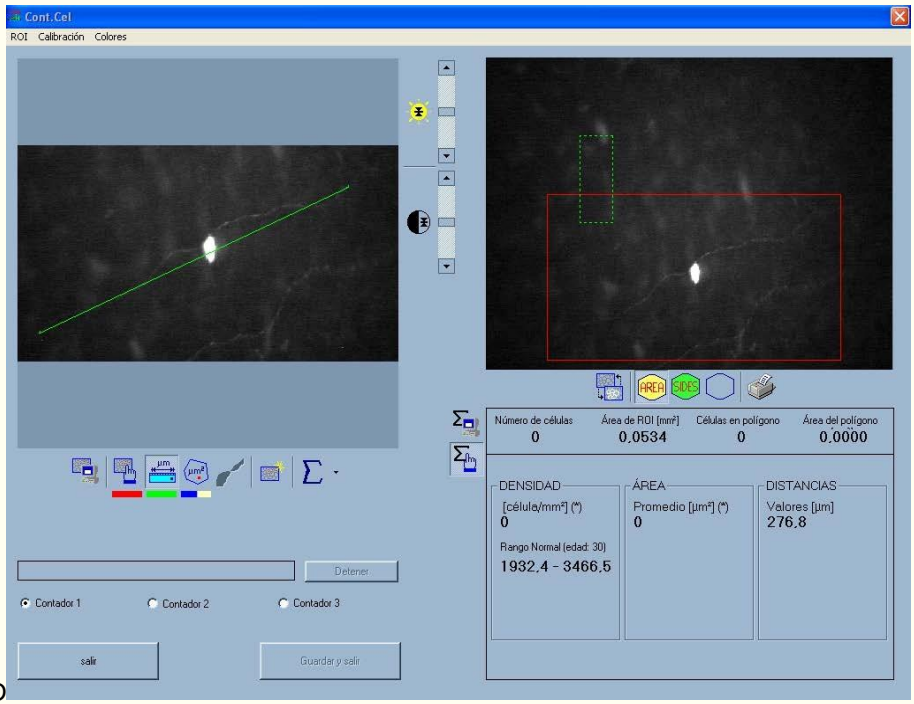

D

Conclusions

The corneal study by confocal microscopy allows the differentiation of epithelium sublayers, subbasal nerve plexus, keratocytes, stromal nerves, and corneal endothelium cells.
Its usefulness has been demonstrated in the study of patients with corneal dystrophies, keratoconus, infectious keratitis, corneal refractive surgery, it has also shown usefulness in the study of patients with corneal transplantation, corneal crosslinking, diabetics, vitrectomized, as well as the study of the filtering bulla in glaucoma.
It is necessary to continue improving the methods of calculation and identification of structures by cornea confocal microscopy, in order to obtain better images and analyzes that contribute to more accurate diagnoses and broaden the spectrum utility of this novel technology.

Conflict of Interest

I confirm there are no conflicts of interest.

References

1. Martínez R, Iviricu R, Correa O, Blanco A, Acosta L. Frecuencia de ametropías diagnosticadas en consulta de cirugía refractiva. Rev CIGET Pinar del Río. 2008;10(3).
2. Tomita M, Kanamori T, Waring GO, Yukawa S, Yamamoto T, Sekiya K, et al. Simultaneous corneal inlay implantation and laser in situ keratomileusis for presbyopia in patients with hyperopia, myopia, or emmetropia: Six- month results. J Cataract & Refract Surg. 2012;38(3):495-506.
3. Christopoulos V, Kagemann L, Wollstein G, Ishikawa H, Gabriele M, Wojtkowski M, et al. In vivo corneal high-speed, ultra–high-resolution optical coherence tomography. Arch Ophthalmol. 2007;125(8):1027-35.
4. Alió JL. Laser refractive surgery: have we arrived? Br J Ophthalmol. 2012;96(9):1159.
5. Winkler C, Khoramnia R, Salgado J, Wullner C, Donitzky C, Mathias M, et al. First clinical results with a new 200 kHz femtosecond laser system. Br J Ophthalmol. 2012;96(6):788-92.
6. Miri A, Alomar T, Nubile M, Al-Agaba M, Lanzini M, Fares U, et al. In vivo confocal microscopic findings in patients with limbal stem cell deficiency. Br J Ophthalmol. 2012;96(4):523-29.
7. Zhivov A, Guthoff RF, Stachs O. In vivo confocal microscopy of the ocular surface: from bench to bedside and back again. Br J Ophthalmol. 2010;94(12):1557-58.
8. Erie JC, McLaren JW, Patel SV. Confocal microscopy in ophthalmology. Am J Ophthalmol. 2009;148(5):639-4.
9. Miri A, Al-Agaba M, Muneer A, Fares U, Said D, Faraj LA, et al. In vivo confocal microscopic features of normal limbus. Br J Ophthalmol. 2012;96(4):530-36.
10. Tavakoli M, Hossain P, Malik RA. Clinical applications of corneal confocal microscopy. Clinical Ophathalmology. 2008;2(2):435-45.
11. Zhivov A, Stachs O, Stave J, Guthoff RF. In vivo three-dimensional confocal laser scanning microscopy of corneal surface and epithelium. Br J Ophthalmol. 2009;93(5):667-72.
12. Villani E, Galimberti D, Viola F, Ratiglia R. In vivo confocal microscopy of the ocular surface. Am J Ophthalmol. 2010;149(4):689-90.
13. Kobayashi A, Mawatari Y, Yokogawa H, Sugiyama K. In vivo laser confocal microscopy after descemet stripping with automated endothelial keratoplasty. Am J Ophthalmol. 2008;145(6):977-85.
14. Guthoff RF, Zhivov A, Stachs O. In vivo confocal microscopy, an inner vision of the cornea - a major review. Clin Experiment Ophthalmol. 2009;37(1):100-17.
15. Petroll WM, Cavanagh HD. Remote-Controlled scanning and automated confocal microscopy through-focusing using a modified HRT Rostock Corneal Module. Eye Contact Lens. 2009;35(6):302-08.
16. Javaloy J, Vidal MT, Ruiz JM, Alió JL. Microscopía confocal de la córnea en la cirugía foforrefractiva. Arch Soc Esp Oftalmol. 2005;80(9):497-509.
17. Ramírez M, Martínez Y, Naranjo R. Hallazgos mediante microscopía confocal en pacientes postoperados de LASIK tratados con antiinflamatorios no esteroideos (AINES). Rev Mex Oftalmol. 2008;82(6):349-51.
18. Nubile M, Mastropasqua L. In vivo confocal microscopy of the ocular surface: where are we now? Br J Ophthalmol 2009;93(7):850-52.

19. Reynolds A, Moore JE, Naroo SA, Moore T, Shah S. Excimer laser surface ablation - a review. Clin & Experiment Ophthalmol. 2010;38(2):168-82.
20. Reinstein DZ, Threlfall WB, Cook R, Cremonesi E, Sutton H, Archer T, et al. Short term LASIK outcomes using the Technolas 217C excimer laser and Hansatome microkeratome in 46 708 eyes treated between 1998 and 2001. Br J Ophthalmol. 2012; 96(9):1173-79.
21. Mastropasqua L, Nubile M, Lanzini M, Carpineto P, Ciancaglini M, Pannellini T, et al. Epithelial dendritic cell distribution in normal and inflamed human cornea: in vivo confocal microscopy study. Am J Ophthalmol. 2006;142(5):736-44.
22. Nishida T. The cornea: stasis and dynamics. Nihon Ganka Gakkai Zasshi.2008;112(3):179-212.
23. Sherwin T. Corneal epithelial homeostasis. Ophthalmology. 2010;117:190-91.
24. Reichard M, Hovakimyan M, Wree A, Meyer A, Nolte I, Junghans C. Comparative in vivo confocal microscopical study of the cornea anatomy of different laboratory animals. Curr Eye Res. 2010;35(12):1072-80.
25. DelMonte DW, Kim T. Anatomy and physiology of the cornea. J Cataract Refract Surg. 2011;37(3):588-98.
26. Mootha V, Dawson D, Kumar A, Gleiser J, Qualls C, Albert DM. Slitlamp, specular, and light microscopic findings of human donor corneas after laser-assisted in situ keratomileusis. Arch Ophthalmol. 2004;122(5):686-92.
27. Ivarsen A, Fledelius W, Hjortdal J. Three-year changes in epithelial and stromal thickness after PRK or LASIK for high myopia. Invest. Ophthalmol. Vis. Sci. 2009;50(5):2061-66.
28. Dvorscak L, Marfurt C. Age-related changes in rat corneal epithelial nerve density. Invest Ophthalmol Vis Sci. 2008;49(3):910-16.
29. Pérez-Gómez I, Efron N. Change to corneal morphology after refractive surgery (myopic in situ keratomileusis) as viewed with a confocal microscope. Optom Vis Sci. 2003;80(10):690-97.
30. Cruzat A, Zheng L, Hamrah P. In vivo confocal microscopy study of epithelial dendritic cells and subbasal nerve plexus in infectious keratitis. 26th Biennial Cornea Conference Abstracts 2009;Boston, MA.
31. Deng SX, Seipal KD, Tang Q, Aldave AJ, Lee O, Yu F. Characterization of limbal stem cell deficiency by in vivo laser scanning confocal microscopy: a microstructural approach. Arch Ophthalmol. 2012;130(4):440-45.
32. Masters BR, Böhnke M. Three-dimensional confocal microscopy of the living human eye. Annu Rev Biomed Eng. 2002;4:69-91.
33. Patel DV, Sherwin T, McGhee CH. Laser scanning in vivo confocal microscopy of the normal human corneoscleral limbus. Invest. Ophthalmol. Vis. Sci. 2006;47(7):2823-27.
34. Barbaro V, Ferrari S, Fasolo A, Pedrotti E, Marchini G, Sbabo A, et al. Evaluation of ocular surface disorders: a new diagnostic tool based on impression cytology and confocal laser scanning microscopy. Br J Ophthalmol 2010;94(7):926-32.
35. Ehlers N, Heegaard S, Hjortdal J, Ivarsen A, Nielsen K, Prause JU. Morphological evaluation of normal human corneal epithelium. Acta Ophthalmology. 2010;88(8):858-61.
36. Ivarsen A, Laurberg T, Møller-Pedersen T. Characterisation of corneal fibrotic wound repair at the LASIK flap margin. Br J Ophthalmol. 2003;87(10):1272-78.

37. Kobayashi A. In vivo laser confocal microscopic analysis of the interface between Bowman's layer and the stroma of the cornea. Nihon Ganka Gakkai Zasshi. 2008;112:947-52.
38. Scarpa F, Zheng X, Ohashi Y, Ruggeri A. Automatic evaluation of corneal nerve tortuosity in images from in vivo confocal microscopy. Invest. Ophthalmol. Vis. Sci. 2011;52(9):6404-08.
39. Zhivov A, Blum M, Guthoff R, Stachs O. Real-time mapping of the subepithelial nerve plexus by in vivo confocal laser scanning microscopy. Br J Ophthalmol. 2010;94(9):1133-35.
40. Allgeier S, Zhivov A, Eberle F, Koehler B, Maier S, Bretthauer G, et al. Image reconstruction of the subbasal nerve plexus within vivo confocal microscopy. Invest. Ophthalmol. Vis. Sci. 2011;52(9):5022-28.
41. Patel SV, McLaren JW, Kittleson KM, Bourne WM. Subbasal nerve density and corneal sensitivity after laser in situ keratomileusis femtosecond laser vs mechanical microkeratome. Arch Ophthalmol. 2010;128(11):1413-19.
42. Erie EA, McLaren JW, Kittleson KM, Patel SV, Erie JC, Bourne W. Corneal subbasal nerve density: A comparison of two confocal microscopes. Eye Contact Lens. 2008;34(6):322-25.
43. Cruzat A, Pavan-Langston D, Hamrah P. In vivo confocal microscopy of corneal nerves: analysis and clinical correlation. Semin Ophthalmol. 2010;25(5):171-77.
44. Grupcheva CN, Wong T, Riley AF, McGhee CN. Assessing the sub-basal nerve plexus of the living healthy human cornea by in vivo confocal microscopy. Clin Experiment Ophthalmol. 2002;30(3):187-90.
45. Esquenazi S, He J, Li N, Bazan NG, Esquenazi I, Bazan HE. Comparative in vivo high-resolution confocal microscopy of corneal epithelium, sub- basal nerves and stromal cells in mice with and without dry eye after photorefractive keratectomy. Clin Experiment Ophthalmol. 2007;35(6):545-
46. Pacheco C, Baca O, Velasco R. Reinervación corneal y dinámica de queratocitos posterior a queratoplastía penetrante. Reporte de casos. Rev Mex Oftalmol. 2008;82(4):263-66.
47. Patel DV, McGhee CN. In vivo laser scanning confocal microscopy confirms that the human corneal sub-basal nerve plexus is a highly dynamic structure. Invest Ophthalmol Vis Sci. 2008;49(8):3409-12.
48. Mimura T, Amano S, Yokoo S, Uchida S, Usui T, Yamagami S. Isolation and distribution of rabbit keratocyte precursors. Mol Vis. 2008;14:197-203.
49. Weaving L, Mihelec M, Storen R, Sosic D, Grigg JR, Patrick PL, et al. Twist2: Role in corneal stromal keratocyte proliferation and corneal thickness. Invest. Ophthalmol. Vis. Sci. 2010;51(11):5561-70.
50. Javadi M, Mozhgan K, Manijeh M, Mehdi Y, Hosein R, Atefeh J, et al. Comparison of keratocyte density between keratoconus, post-laser in situ keratomileusis keratectasia, and uncomplicated post-laser in situ keratomileusis cases. A confocal scan study. Cornea. 2009;28(7):774-79.
51. Argento C, Croxatt JO. Evaluación de la celularidad estromal corneal mediante microscopía confocal en LASEK con Mitomicina. Oftalmol Clin Exp. 2007;35(1):14-20.
52. Niederer RL, McGhee CN. Clinical in vivo confocal microscopy of the human cornea in health and disease. Prog Retin Eye Res. 2010;29(1):30.
53. Zhao Ch, Lu S, Tajouri N, Dosso A, Safran A. In vivo confocal laser scanning microscopy of corneal nerves in leprosy. Arch Ophthalmol. 2008;126(2):282-84.
54. Marfurt CF, Deek S, Dvorscak L. Anatomy of the human corneal innervation. Exp Eye Res. 2010;90:478-92.

55. Al-Faky Y, Bosley T, Turki T, Salih M, Abu-Amero K, Alsuhaibani A. Prominent corneal nerves: a novel sign of lipoid proteinosis. Br J Ophthalmol. 2012;96(7):935-40.
56. Al-Aqaba MA, Fares U, Suleman H, Lowe J, Dua HS. Architecture and distribution of human corneal nerves. Br J Ophthalmol. 2010;94(6):784-89.
57. Karagianni N, Fukuoka S. Analysis of corneal nerve regeneration following deep vs. superficial injury. ARVO Meeting Abstracts. 2010;51:392.
58. Jiucheng H, Bazan N, Bazan H. Mapping the entire human corneal nerve architecture. Exp Eye Res. 2010;91(4):513-23.
59. Vanathi M, Tandon R, Sharma N, Titiyal JS, Pandey RM, Vajpayee RB. In-vivo slit scanning confocal microscopy of normal corneas in Indian eyes. Indian J Ophthalmol. 2003;51(3):225–30.
60. Patel SV, Bourne W. Corneal endothelial cell loss 9 years after excimer laser keratorefractive surgery. Arch Ophthalmol. 2009;127(11):1423-27.
61. Lagali N, Dellby A, Fagerholm P. In vivo confocal microscopy of the cornea in Darier-White disease. Arch Ophthalmol. 2009;127(6):816-18.
62. Lautebach S, Funk J, Reinhard T, Pache M. Steroid glaucoma after laser in situ keratomileusis. Klin Monatsbl Augenheilkd. 2007; 224(5):438-40.
63. Jareño Ochoa M, Pérez Parra Z, Fernández García K, Castillo Pérez A, Escalona Leyva E, Ruíz Rodríguez Y. Changes in the cell structure of patients with keratoconus under cross-linking treatment by using confocal microscopy. Rev Cubana Ophthalmology. 2012; 25 (2).
64. Pérez Parra Z, Padilla González C, Jareño Ochoa M, Gómez Castillo Z, Guerra Almaguer M, Sibila González M. Corneal changes after penetrating optical keratoplasty. Rev Cubana Ophthalmology. 2017; 30 (1).
65. González–Sotero J, Casanueva-Cabeza HC, Alberro-Hernández M, Rojas-Alvarez E. Microscopía confocal en las distrofias corneales. ARCH. OFTAL. B. AIRES; vol 82 nº 1; pág 33-39; 2011.
66. Rojas Alvarez E, González Sotero J. Sequential confocal microscopy of corneal nerve regeneration in myopia surgery by PRK. Rev Mex Oftalmol . 2018; 92 (3).
67. Rojas-Alvarez E, González-Sotero J. Quantitative confocal microscopy of corneal haze and correlation with the ametropy to be treated, in surface refractive surgery. Rev Mex Oftalmol 2016;90:159-66.
68. Rojas-Alvarez E, González-Sotero J. Tamargo Barbeíto T. Corneal morphometric predictive models from ametropia to excimer laser treatment. Arch Soc Esp Oftalmol 2015;90:312-23.
69. Rojas-Alvarez E, González-Sotero J (2013). LASIK vs. LASEK: in vivo corneal morphometrical perspective. Rev Mex Oftalmol 2013; 87(3): 145 – 157. 2013.
70. Álvarez Marín J, Rodríguez Gil R, Alfonso Rodríguez A, Abreu Reyes p. Application of confocal microscopy in the diagnosis of Acanthamoeba keratitis. Archivos de la Sociedad Canaria de Oftalmología. 2011; 22: 14-19.
71. Veitía Rovirosa ZN, García Ramos L, Bauza Fortunato Y, Pérez Candelaria EC, Rodríguez Suárez B, Méndez Duque de Estrada AM. Use of the confocal microscopy in patients vitrectomized with silicone oil in their anterior chamber. Rev Cubana Ophthalmology. 2014; 27 (2).
72. Gutiérrez Castillo M, Castillo Pérez AC, Ramos López M, Pérez Parra Z, Ramos Pereira Y, Barroso Lorenzo R. Confocal microscopy of the cornea in diabetic patients. ReV Cubana de Ophthalmology. 2020;33(1)e692.
73. Ferrer Guerra MT, Díaz Águila Y, Fernández Argones L, Piloto Díaz I, Domínguez Randulfe M, Obret Mendive I. Confocal laser scanning microscopy and its association to the morphology of the filtering bleb. Rev Cubana Ophthalmology. 2012; 25 (2).